Arab J Sci Eng (2017) 42:1505–1515
DOI 10.1007/s13369-016-2363-4

RESEARCH ARTICLE - CHEMICAL ENGINEERING

Energetic Performance Optimization of a SOFC–GT Hybrid Power Plant

Salha Faleh[1] · **Tahar Khir**[1] · **Ammar Ben Brahim**[1]

Received: 9 June 2016 / Accepted: 17 November 2016 / Published online: 7 December 2016
© King Fahd University of Petroleum & Minerals 2016

Abstract Analytic study based on energy analysis is conducted on a solid oxide fuel cell (SOFC) integrated in a gas turbine power plant GT. The Tunisian natural gas is used as fuel for the SOFC and the GT cycle. An external pre-reforming system is installed before the SOFC. Heat recovery systems are adopted to valorize the waste heat at the SOFC and GT exhausts. The gas from the SOFC exhaust is also used as additional supply of the combustion chamber. The equations governing the electrochemical processes and the energy balances of the power plant components are established. Numerical simulations using EES software are performed. The influences of key operating parameters, such as ambient temperature, air flow, pre-reforming fraction and fuel utilization on the performance of the SOFC–GT hybrid system, are analyzed. The integration of the SOFC enhances the hybrid cycle efficiency of about 50%. The increase of the ambient temperature reduces the system efficiencies. The utilization factor has a negative effect on the SOFC temperature and voltage which leads to a decrease in the system performances, while the pre-reforming fraction has a positive effect on the indicated parameters. The SOFC voltage increases with the air molar flow rate. However, required air compressor power becomes important. That reduces significantly the SOFC efficiency. A small improvement of about 2% is obtained for the hybrid cycle efficiency SOFC–GT.

Keywords Gas turbine · SOFC · Hybrid system · Natural gas · Pre-reforming · Polarization · Utilization factor · Ambient temperature

List of symbols

SOFC	Solid oxide fuel cell
GT	Gas turbine
HE	Heat exchanger
V_{ohm}	Ohmic polarization (V)
V_{act}	Activation polarization (V)
V_{conc}	Concentration polarization (V)
I	Current density (A/m^2)
R_{e}	The resistance (Ω)
δ_j	The thickness (m)
ρ_j	The specific electric resistivity of the anode, cathode, electrolyte and interconnect
A_j	The area (m^2)
ε	The porosity coefficient
τ	The tortuosity coefficient
$D_{1,K}$	The Knudsen diffusion coefficient
σ_{12}	Collision diameter
Ω_{12}	Collision integral
PR	The pressure ratio
k	The specific heat ratio
$\dot{m}_{\mathrm{a}}$	The mass of dry air the ratio (kg/s)
$\dot{m}_{\mathrm{v}}$	The mass of vapor (kg/s)
$\dot{m}_{\mathrm{f}}$	The mass of fuel (kg/s)
T_{am}	Ambient temperature (°C)
η	Energetic efficiency
U_{f}	Utilization factor
V_{SOFC}	SOFC voltage (V)
X_{reform}	Pre-reforming fraction
$\dot{\eta}_{\mathrm{air}}$	Air flow (mol/s)

✉ Salha Faleh
elfaleh.s@gmail.com

[1] Applied Thermodynamic Research Unit UR11ES80, National Engineering School of Gabes, Omar Ibn elKhattab Street, 6029 Gabès, Tunisia

η_c	Isentropic efficiency
P_{SOFC}	SOFC power output (MW)
W_{GT}	Gas turbine power output (MW)
W_{aux}	Auxiliary power (MW)

1 Introduction

Hybrid SOFC–GT plants are promising power generation systems of high efficiency. SOFC converts the free energy change of a chemical reaction directly into electrical energy, and it is effluent at high temperature which makes it suitable for integration with gas turbine cycles. SOFC technology has attracted considerable interest. It is demonstrated by simulation technique that SOFC can achieve 50% net electrical efficiencies and considered feasible for integration with multi-MW gas turbine engines to achieve considerably high electrical efficiency [1]. Barelli et al. [2] studied heat recuperation from the turbine exhaust gas to heat the air inlet of SOFC, producing steam and heating for the steam reformer using recuperative heat exchanger with 10% thermal power loss.

El-Emam et al. [3] developed an energy and exergy analyses of an integrated gasification and solid oxide fuel cell (SOFC) system with a gas turbine and steam cycle using heat recovery of the gas turbine exhaust. They found for two different types of coals, an energy efficiency of the overall system equal to 38.1 and 36.7%, and an exergy efficiency equal to 27 and 23.2%.The combination of two or more power cycles into one system is a practical option for efficient power generation and for improving the overall performance of the energy conversion system and the energy efficiency [4,5]. Solid oxide fuel cell (SOFC) technology is a promising technology to work in integrated plants due to its high operating efficiency, solid-state design, operating conditions and high-temperature capability and the potential for gas and liquid fuel internal reforming [6,7]. Penyarat [8] proposed and simulated in MATLAB few configurations of the combined or hybrid cycles to select the better configuration.

Yi et al. [9] applied design of experiments (DOEx) approach to the hybrid system (The solid oxide fuel cell and intercooled gas turbine SOFC–ICGT hybrid cycle). They found that operating under a high operating pressure (50 bars) and with a low percent excess air (55%) in the SOFC, system electrical efficiency higher than 75% (net ac/lower heating value (LHV)) can be achieved. Inui et al. [10] proposed a fossil fueled SOFC/GT system reaching 70.64% as total thermal efficiency. Chan et al. [11] studied the effects of operating pressure and fuel flow rate on the performance of the components and overall SOFC/GT hybrid system. They concluded that an electrical efficiency of more than 60% could be achieved using an internal-reforming hybrid SOFC/GT system. Massardo et al. [12] reported that 50% net electrical efficiencies can be obtained using SOFC which can be integrated with multi-MW gas turbine to rise electrical efficiency. Arsalis [13] noted that for a realistic system, gas turbine and steam turbine are very inefficient at small sizes 1.5 MWe SOFC–GT–ST comparing to 5 or 10 MW system. Ishak [14] presents the integration of direct ammonia solid oxide fuel cell with a gas turbine. This study is conducted to investigate the effects of varying the operating conditions and parameters on the energy and exergy efficiencies and the overall system performance. Penyarat et al. [15] developed a hybrid solid oxide fuel cell and gas turbine power system models based on simple thermodynamic expressions. They conclude that fuel cell performance is a strong function of operating temperature and that cycle performance depends on SOFC temperature and the exhaust temperature.

Zhang etal. [16] proposed many system integration schemes for coupling SOFC stacks with various bottoming cycles depending on the application. An interest review conducted by Zamfirescu and Dincer [17] presented a combined system (hydrogen-fed integrated SOFC/GT) for vehicular applications. They found that in maximum efficiency, fuel cell reduces the compactness by 40%. It was also found that 60% of total exergy destruction in the system occurred at the fuel cell stack.

Dang et al. [18] proposed the anode and cathode exhaust gas recirculation to enhance the efficiency of SOFC–GT hybrid system. They found that the recirculation has a direct impact on gas turbine efficiency and it assures the highest system and thermal efficiency.

In this study, an energy optimization of SOFC–GT hybrid cycle was investigated. An appropriate design of the power plant is considered. That permits to valorize the waste heat and matter fluxes. The effects of key parameters such as ambient temperature, air flow, pre-reforming fraction and utilization factor on the performance of simple cycle and hybrid cycle were analyzed.

2 System Description

Schematic diagram of the considered power plant is shown in Fig. 1. It is mainly constituted by compressors, heat exchangers, solid oxide fuel cell, combustion chamber and gas turbine. The input air and fuel streams of fuel cell are preheated by means of heat exchangers using recovered heat from re-circulated gas turbine exhaust mixture. The fuel outlet temperature is controlled by adjusting the mass flow of the stream in order to fulfil the requirement of the SOFC inlet temperature. For the air stream, the air pressure is firstly raised in the air compressor and then the air is preheated in a heat exchanger. The needed water is generated in the steam generator where the exhaust heat from HE1 is again utilized to heat the water from the pump. Fuel is firstly partially pre-

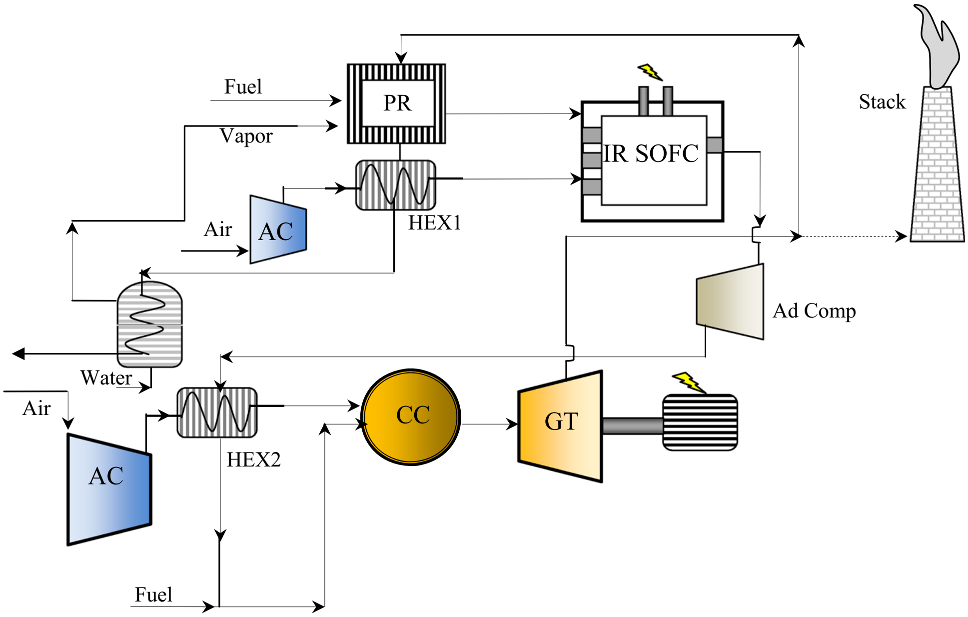

Fig. 1 Schematic diagram of the considered power plant

Table 1 Characteristic designs of the SOFC GT hybrid cycle

Parameters	Values
Compressor isentropic efficiency (%)	90
Recuperator effectiveness (%)	90
GT pressure ratio	10
Turbine isentropic efficiency (%)	94
Cell length (cm)	150
Cell outside diameter (cm)	2.2
Cell voltage (V)	0.6
DC–AC converter efficiency (%)	95
Limiting current density (mA/cm^2)	300

reformed using the pre-reformer than it is reformed in the SOFC. The chemical energy is converted to the electrical energy through the electrochemical reaction taking place in the SOFC. Exhaust flow from the cell passes through the combustor chamber where the residual hydrogen and hydrocarbon are burned. The SOFC exhaust heat is utilized before in the recuperator to heat the compressor discharge air flowing to the gas turbine. The main characteristic designs of the SOFC GT hybrid cycle are given in Table 1.

3 Mathematical Model

3.1 SOFC

The fuel cell model developed in this study is based on a tubular design. The sizes of the different elements and the material choice are selected according the available data [19].

A zero-dimensional model is implemented which calculates the stack power and outlet stream parameters at the stack temperature.

Proposed model represents a natural gas fueled system. The SOFC can be fueled by hydrogen or directly by hydrocarbon without the need of pre-reforming [20]. It is commonly considered that reforming, shifting and electrochemical reactions are taken place inside the cell.

3.1.1 Electrochemical Model

The electrochemical reactions around the anode and the cathode are:

$$\text{Anode side: } H_2 + O^{2-} \rightarrow H_2O + 2e^- \tag{R1}$$

$$\text{Cathode side: } \frac{1}{2}O_2 + 2e^- \rightarrow O^{2-} \tag{R2}$$

$$\text{Overall reaction: } H_2 + \frac{1}{2}O_2 \rightarrow H_2O \tag{R3}$$

The theoretical open circuit cell voltage E_{th} can be determined by the Nernst equation as:

$$E_{\text{th}} = E^\circ + \frac{RT_P}{neF}\text{Ln}\frac{P_{H_2}P_{O2}^{1/2}}{P_{H_2O}} \tag{1}$$

The real cell voltage is less than theoretical one. The losses called polarizations are mainly due to ohmic overpotential, activation overpotential and concentration overpotential.

Table 2 Ohmic polarization constants

Composant	$A(\Omega - m)$	B (K)	δ (m)
Cathode	0.0000811	600	0.0022
Anode	0.0000298	−1392	0.0001
Electrolyte	0.0000294	10,350	0.00004
Inter-connector	0.0012	4690	0.000085

Hence, the actual voltage of an operating fuel cell is given by:

$$E_r = E_{th} - V_{ohm} - V_{act} - V_{conc} \tag{2}$$

a. Ohmic overpotential

Ohmic losses V_{ohm} arise from the resistance to charge conduction through the various cell components. These losses are due firstly to the electronic conduction occurring in the electrodes and the inter-connector and secondly to the ionic conduction of oxygen and anions through the solid electrolyte. The ohmic losses may be expressed as:

$$V_{ohm} = I.R_e = I.\sum_j \rho_j \delta_j \tag{3}$$

$$\rho_j = A_i \exp\left(\frac{B_i}{T}\right) \tag{4}$$

The values of the constant parameters indicated in this equation are given in Table 2.

b. Concentration overpotential

The electrochemical reactions occur at the electrolyte–electrode interface. However, the considered gas partial pressures, used to calculate the change of Gibbs free energy, are different from the values really obtained in the reactions. So, corrections are usually performed to determine the Gibbs free energy at both the anode and the cathode. These corrections obtained by the concentration polarization V_{conc} are given as follows:

$$V_{conc,an} = \frac{RTp}{neF} \mathrm{Ln}\left(\frac{1 - \frac{i}{i_{l,H_2}}}{1 + \frac{i}{i_{l,H_2O}}}\right) \tag{5}$$

$$V_{conc,ca} = \frac{RTp}{nF} \mathrm{Ln}\left(\frac{1}{1 - \frac{i}{i_{l,O_2}}}\right) \tag{6}$$

$$i_{l,H_2} = \frac{neFD_{eff,H_2}}{RTp\delta an} P_{H_2} \tag{7}$$

$$i_{l,H_2O} = \frac{neFD_{eff,H_2O}}{RTp\delta an} P_{H_2O} \tag{8}$$

$$i_{l,O_2} = \frac{neFD_{eff,O_2}}{RTp\delta ca} P_2 \tag{9}$$

D_{eff}: represents the effective diffusion coefficient, and it can be determined by Bosanquet formula:

$$\frac{1}{D_{eff,1}} = \frac{\varepsilon}{\tau}\left(\frac{1}{D_{1,K}} + \frac{1}{D_{1,2}}\right) \tag{10}$$

$D_{1,K}$: the Knudsen diffusion coefficient for specie 1 is evaluated using free molecule flow theory:

$$D_{1,K} = \frac{2}{3} r_e \left(\frac{8RT}{\pi M_1}\right)^{\frac{1}{2}} \tag{11}$$

$D_{1,2}$: the diffusion coefficient for gas pairs, it is expressed by Hirschfelder equation as

$$D_{1,2} = \frac{1.858 * 10^{-27} * T^{\frac{3}{2}}}{P * \sigma_{12}^2 * \Omega_{12}} \left(\frac{1}{M_1} + \frac{1}{M_2}\right)^{1/2} \tag{12}$$

c. Activation overpotential

Chemical reactions, including electrochemical reactions, involve energy barriers which must be overcome by the reacting species. This energy barrier is called "activation energy" and results in activation or charge- transfer polarization, which is due to the transfer of charges between the electronic and the ionic conductors. The activation polarization V_{act} represents the potential necessary to overcome the energy barrier related to the electrode reaction. V_{act} is determined using the Butler–Volmer equation [21] as follows:

$$i = i_0 \left[\exp\left(\frac{\beta F n_e V_{act}}{RT_p}\right) - \exp\left(-\frac{(1-\beta) F n_e V_{act}}{RT_p}\right)\right] \tag{13}$$

where β is usually taken equal to 0.5. That permits to express V_{act} by:

$$V_{act} = \frac{2RT_p}{neF} \sinh^{-1}\left(\frac{i}{2i_0}\right); \tag{14}$$

where i_0 is the exchange current density, depending on the partial pressure of the reacting gas, compositions and the temperature.

At the anode side, the exchange current density is given by:

$$i_{0,an} = \gamma_a \left(\frac{P_{H_2}}{P_0}\right)\left(\frac{P_{H_2O}}{P_0}\right) \exp\left(-\frac{E_a}{RT_p}\right) \tag{15}$$

While at cathode side it is expressed as follows:

$$i_{0,ca} = \gamma_c \left(\frac{P_{O_2}}{P_0}\right)^{0.25} \exp\left(-\frac{E_a}{RT_p}\right) \tag{16}$$

Table 3 Activation polarization constants

$E_{\mathrm{act,an}}$ (kJ kmol^{-1})	110,000
$E_{\mathrm{act,ca}}$ (kJ kmol^{-1})	155,000
$\gamma^{\mathrm{an,ca}}$ (A/m^2)	7×10^9

The values of the different constants in Eqs. (15) and (16) are given in Table 3.

3.1.2 Internal Reforming and Shifting Models

The SOFC is flexible regarding the use of different types of fuel. In fact SOFC can be fed not only by hydrogen but also by several hydrocarbons and carbon monoxide. The SOFC operating temperature is high enough to enable the direct reformation of natural gas. The hydrogen is electrochemically converted with production of electrical power and high-grade waste heat for recuperation [13].

The reforming and water gas shift reactions occur within the anode as follows:

$$\text{Steam reforming reaction:}\quad CH_4 + H_2O \rightarrow CO + 3H_2 \tag{R4}$$

$$\text{Shifting reaction:}\quad CO + H_2O \rightarrow CO_2 + H_2 \tag{R5}$$

In addition, the carbon monoxide electrochemical oxidation is obtained at the anode according to the following reaction.

$$CO + O^{2-} \rightarrow CO_2 + 2e^- \tag{R6}$$

But, seeing that its velocity is 2–5 times slower than that of hydrogen, this reaction is generally neglected. Consequently, the rapid water gas shift reaction becomes the dominant one.

The equilibrium constants of reforming and shifting reactions can be evaluated by:

$$Kp_{\mathrm{r}} = \frac{p^3_{H_2} p_{CO}}{p_{CH_4} p_{H_2O}} = \frac{\left[\left(CO^0 + x - y\right) / \left(n^0_{\mathrm{tot}} + 2x\right)\right] * \left[\left(H^0_2 + 3x + y - z\right)^3 / \left(n^0_{\mathrm{tot}} + 2x\right)^3\right]}{\left[\left(CH^0_4 - x\right) / \left(n^0_{\mathrm{tot}} + 2x\right)\right]\left[\left(H_2O^0 - x - y + z\right) / \left(n^0_{\mathrm{tot}} + 2x\right)\right]} p^2_{\mathrm{cell}} \tag{17}$$

$$Kp_{\mathrm{s}} = \frac{p_{H_2} p_{CO_2}}{p_{CO} p_{H_2O}} = \frac{\left[\left(CO^0_2 + y\right) / \left(n^0_{\mathrm{tot}} + 2x\right)\right] * \left[\left(H^0_2 + 3x + y - z\right)^3 / \left(n^0_{\mathrm{tot}} + 2x\right)^3\right]}{\left[\left(CO^0 + x - y\right) / \left(n^0_{\mathrm{tot}} + 2x\right)\right]\left[\left(H_2O^0 - x - y + z\right) / \left(n^0_{\mathrm{tot}} + 2x\right)\right]} \tag{18}$$

$$z = U_{\mathrm{f}} * (3x + y) \tag{19}$$

$$\mathrm{Log}\,(Kp) = AT^4 + BT^3 + CT^2 + DT + E \tag{20}$$

For this study, the fuel used to supply the SOFC and the GT cycle is the Natural Tunisian Gas NTG. The chemical properties of this fuel are reported in Table 5. It is known that the use of Natural gas with internal reforming SOFC may provoke carbon deposition in the anodic electrode. To avoid this phenomenon, a steam to carbon ratio between 1.5 and 2 is considered for the actual analytic study as suggested by several previous works. Furthermore, the use of specific catalyst is proposed as technical solution to prevent the carbon deposition [22].

In order to reduce the CO_2 release, new technical solutions are added to the hybrid SOFC–GT cycle such as the use of specific heat exchangers to convert CO_2 gas to liquid state [23]. Duan et al reported that zero-CO_2 SOFC hybrid systems still have higher efficiencies when compared with the SOFC hybrid system without CO_2 capture. They reported also that SOFC can produce power at high efficiency with the less energy consumption for CO_2 capture [24]. For the present study, the gas flux from the SOFC is valorized by its re-injection into the GT combustion chamber. So, the solutions commonly used for CO_2 capture in the GT cycle may be used.

where x, y and z are the molar flow rate of CH_4, CO and H_2 calculated by solving simultaneously Eqs. (17)–(20). The different constants in equation (d) are given in Table 4.

Calculating of the effluent gas temperature from the SOFC is an important step. The heat generated by the electrochemical reaction is simultaneously used to supply the required heat of the internal reforming reaction and to heat the SOFC products and residual reactants until the stack temperature. But in real systems, a pre-reforming process is applied for which hot gases, from the SOFC, may be used to provide the thermal energy needed for the pre-reforming process.

Table 4 Equilibrium constants of reforming and shifting reactions [25]

	Reforming	Shifting
A	-2.63121×10^{-11}	5.47301×10^{-12}
B	1.24065×10^{-7}	-2.57479×10^{-8}
C	-2.25232×10^{-4}	4.63742×10^{-5}
D	1.95028×10^{-1}	-3.91500×10^{-2}
E	-6.61395×10^{1}	1.32097×10^{1}

3.2 Gas Turbine

The hot gaseous mixture leaving the combustion chamber expands through the gas turbine to deliver useful power. Turbine is used to drive simultaneously the electrical generator and the air compressor.

The turbine outlet temperature can be determined by:

$$\frac{T_{\mathrm{out}}}{T_{\mathrm{in}}} = \mathrm{PR}^{\frac{k-1}{k}}; \tag{21}$$

Taking into consideration the turbine isentropic efficiency η_{is}, the produced power is calculated by

$$\dot{W}_{\mathrm{t}} = \eta_{\mathrm{is}} \dot{m}_{\mathrm{t}} C_{\mathrm{pg}} \left(T_{\mathrm{in}} - T_{\mathrm{out}}\right) \tag{22}$$

where $\dot{m}_{\mathrm{t}}$ is the total mass flow rate given by:

$$\dot{m}_{\mathrm{t}} = \dot{m}_{\mathrm{a}} + \dot{m}_{\mathrm{v}} + \dot{m}_{\mathrm{f}} \tag{23}$$

3.3 Combustion Chamber

Three streams are used to feed the combustion chamber as indicated in Fig. 1: the compressed air, the fuel and the SOFC exhaust gas including the unreacted hydrogen hydrocarbure and other effluents including excess air. The reactions occurring in combustion chamber are:

$$\mathrm{CH_4 + 2O_2 \rightarrow CO_2 + 2H_2O} \tag{R7}$$

$$\mathrm{C_2H_6} + \frac{7}{2}\mathrm{O_2 \rightarrow 2CO_2 + 3H_2O} \tag{R8}$$

$$\mathrm{C_3H_8 + 5O_2 \rightarrow 3CO_2 + 4H_2O} \tag{R9}$$

$$\mathrm{H_2 + O_2 \quad \rightarrow 2H_2O} \tag{R10}$$

$$\mathrm{CO} + \frac{1}{2}\mathrm{O_2 \rightarrow CO_2} \tag{R11}$$

The fuel supplied the proposed cycle is the Natural Tunisian Gas. Its composition is reported in Table 5.

Table 5 Natural Tunisian Gas composition

	Molar composition (%)
N_2	3.04
CO_2	0.64
CH_4	78.95
C_2H_6	13.5
C_3H_8	3.87

3.4 Compressors

These components receive air at ambient temperature and pressure to be compressed to the desired pressure resulting in an increase in its temperature. Model of the compressor is based on the perfect gas equations and polytropic transformations. The exhaust isentropic temperature is calculated by:

$$\frac{T_{\mathrm{out}}}{T_{\mathrm{in}}} = \left[\frac{P_{\mathrm{out}}}{P_{\mathrm{in}}}\right]^{\frac{k-1}{k}} = \mathrm{PR}^{\frac{k-1}{k}} \tag{24}$$

Mechanical power consumed by the compressor:

$$w_{\mathrm{c}} = \left(\dot{m}_{\mathrm{a}} \Delta H_{\mathrm{c}}\right) / \eta_{\mathrm{c}} \tag{25}$$

Where ΔH_{c} is the isentropic enthalpy variation through the compressor.

$$\Delta H_{\mathrm{c}} = H_{\mathrm{out}} - H_{\mathrm{in}} \tag{26}$$

3.5 Heat Exchangers

In the considered system, multiple gas to gas heat exchangers are used for heat recovery processes. It is assumed that there is no heat transfer between these recuperators and the surrounding environment. The effectiveness- NTU method is used to determine the actual temperature changes for both cold and hot fluids, based on the heat exchanger type, effective heat transfer coefficient and surface area. For a cross-flow and unmixed fluid-type heat exchanger, the effectiveness is expressed as [26]:

$$\epsilon = 1 - \exp\left\{\frac{\mathrm{NTU}^{0,22}}{c}\left[\exp\left(-c\mathrm{NTU}^{0,78}\right) - 1\right]\right\} \tag{27}$$

$$C_{\mathrm{r}} = \frac{C_{\mathrm{min}}}{C_{\mathrm{max}}} \tag{28}$$

$$\mathrm{NTU} = \frac{\mathrm{UA}}{C_{\mathrm{min}}} \tag{29}$$

$$Q_{\mathrm{max}} = C_{\mathrm{min}}\left(T_{\mathrm{in}}^{\mathrm{hot}} - T_{\mathrm{in}}^{\mathrm{cold}}\right) \tag{30}$$

$$Q = \Delta H_{\mathrm{cold}} = -\Delta H_{\mathrm{hot}} = \varepsilon Q_{\mathrm{max}} \tag{31}$$

Overall cycle efficiency

The overall cycle efficiency including the gas turbine cycle and the SOFC system is expressed by:

$$\eta = \frac{\text{Net system Power Output}}{\text{Total Energy input}} \tag{32}$$

The Net system Power Output NPO is expressed by:

$$\mathrm{NPO} = P_{\mathrm{SOFC}} + W_{\mathrm{TG}} - W_{\mathrm{aux}} \tag{33}$$

Table 6 Operating variables ranges

Parameters	Values
Compressor isentropic efficiency (%)	90
Recuperator effectiveness (%)	90
GT inlet temperature (°C)	1200
Expansion ratio	10
Turbine isentropic efficiency (%)	94
Cell length (cm)	150
Cell outside diameter (cm)	2.2
Current density (A/m^2)	3000
Cell voltage (V)	0,6
Cell operating temperature (K)	850–1200
Fuel utilization (%)	60
DC–AC converter efficiency (%)	95
Limiting current density (mA/cm^2)	300
Steam to carbon ratio	1.5–2

The Total Energy Input TEI is given by:

$$\mathrm{TEI} = \mathrm{LHV} * (\dot{m}_{\mathrm{fSOFC}} + \dot{m}_{\mathrm{fGT}}) \quad (34)$$

4 Analytic Study

The performances of the SOFC gas turbine hybrid cycle are determined considering the operating parameters related to the local environmental conditions of the south of Tunisia. The effects of main operating parameters such as the ambient temperature, the air flow rate, the SOFC pressure, the fuel utilization factor and the degree of pre-reforming are analyzed. A code is developed using EES software to perform the required calculations. The operating variables ranges are indicated in Table 6.

5 Results and Interpretations

5.1 Effect of the Ambient Temperature

One of the most important problems effecting power generators behavior is the decrease of power output at high air ambient temperatures, especially in hot season. In fact, as the ambient air temperature increases, the compressed air mass flow rate decreases and to keep it constant, compressors consume more electrical energy, and consequently, the gas turbine and fuel cell output capacities are reduced. In the following section, the effects of ambient temperature on the performance of each system will be analyzed. The modeling was carried out considering a pressure ratio of 10, a pre-reforming fraction of 0.8 and an utilization factor of 0.6.

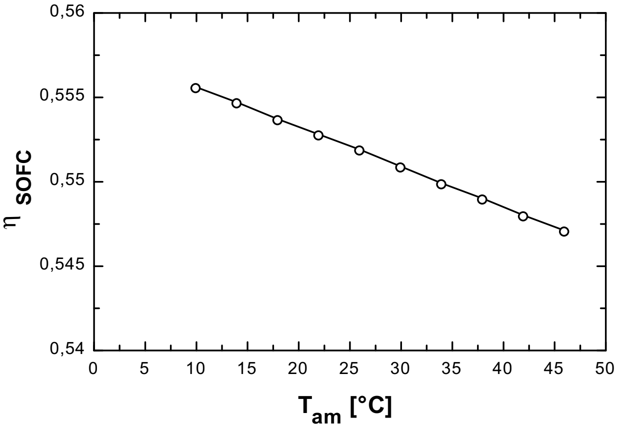

Fig. 2 Effect of ambient temperature on SOFC efficiency

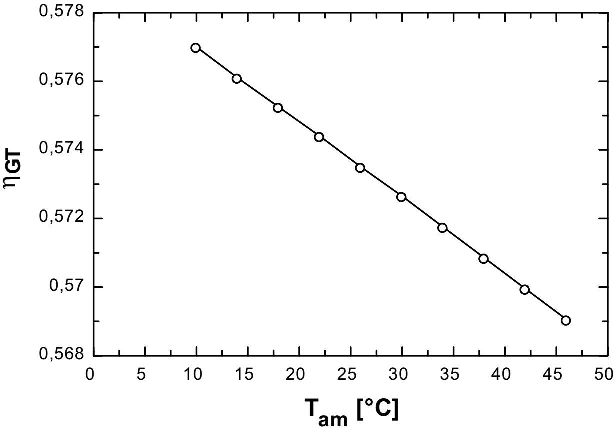

Fig. 3 Effect of ambient temperature on GT efficiency

The ambient temperature does not affect significantly the SOFC energy efficiency as shown in Fig. 2. For the considered ambient temperature variation range, the energy efficiency decreases of about only 1%. The same behavior for the gas turbine energy efficiency variation is observed as depicted in Fig. 3. For this arrangement, the GT cycle performance is enhanced with the fuel mass flow rate issued from the SOCF to reach about 55%, while for a simple GT cycle without SOFC integration the energy efficiency remains relatively small around 40%. The SOFC integration leads to an improvement of the whole system energy efficiency of about 50% as shown in Fig. 4.

5.2 Effect of SOFC Fuel Utilization Factor on System Performance

The utilization factor is an important operating parameter. It is defined as the ratio of the fuel really consumed to the supplied fuel.

Figure 5 represents the effect of utilization factor U_{f} on the SOFC temperature. The results show that the temperature of

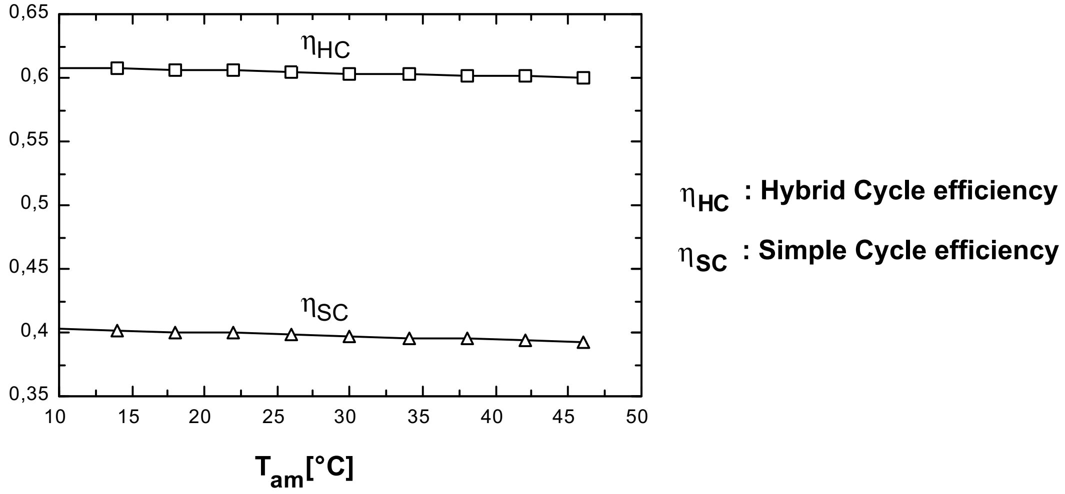

Fig. 4 Effect of ambient temperature on GT, SOFC–GT hybrid system efficiencies

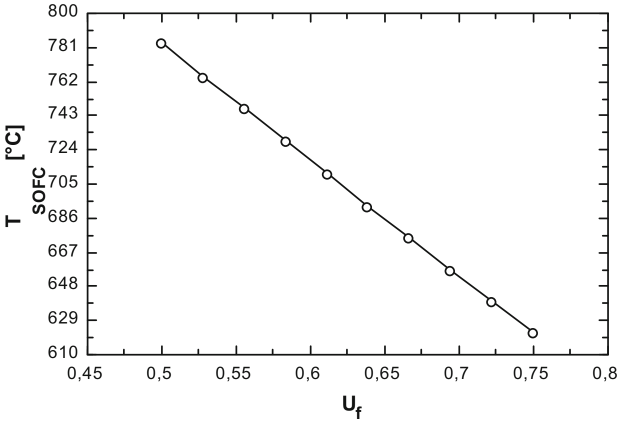

Fig. 5 Effect of fuel utilization on SOFC temperature

SOFC decreases significantly with U_f. For a variation range of U_f from 0.5 to 0.75, the SOFC temperature decreases from 783 to 622.3 °C. This is because more of hydrogen is consumed in the electrochemical reaction.

The efficiency variations of SOFC, GT and SOFC–GT systems are plotted against the fuel utilization factor in Fig. 6. The obtained results show that the efficiencies decrease with the increase of U_f. One can see that the utilization factor has a significant effect on the SOFC efficiency. For the U_f variation range (0.5–0.75), the SOFC efficiency is reduced of about 73%. In fact, this factor determines the number of hydrogen moles consumed in the electrochemical reaction. Really, the system operates with fuel excess to avoid anode oxidation and cell degradation as a result of the concentration gradients of the different species and the chemical stresses. An utilization factor enhancement of 5%, leads to a decrease of SOFC, GT and SOFC–GT efficiencies of about 23.2 and 3%, respectively.

Furthermore increasing the utilization factor causes sensibly reduction of the cell voltage due to internal irreversibility rise as depicted in Fig. 7. Thus, the power produced by the SOFC decreases significantly.

5.3 Effect of Pre-reforming Fraction

The pre-reforming unit consists of a tube bundle filled with a catalyst in an appropriate shell. The reformed gas flows inside the tubes, while the hot gases from the turbine exhaust pass through the shell.

In the purpose to improve the system performances, pre-reforming and internal reforming are combined. Indeed, the internal reforming is beneficial since it ensures the consumption of the unreacted methane and carbon monoxide, while the external reforming is used to crack the long hydrocarbon chains and feed the cell with H_2 in order to bring the operating point and increase the stack efficiency. In this way more available cell surface will be preserved for electrochemical reactions.

To analyze the effect of pre-reforming fraction on the system efficiencies, the modeling was carried out considering the following operating parameters:

- Cell pressure10^3 kPa,
- Ambient temperature 283,15 K
- Utilization factor 0.6.

The variation of the cell temperature according to the pre-reformed fraction X_r is presented in Fig. 8. The cell temperature rises from 629.9 to 751.7 °C for an increase of X_r from 0.5 to 0.9. This is due to the endothermic reforming reaction. Indeed, this reaction requires energy input which reduces the sack temperature. The temperature rising reduces

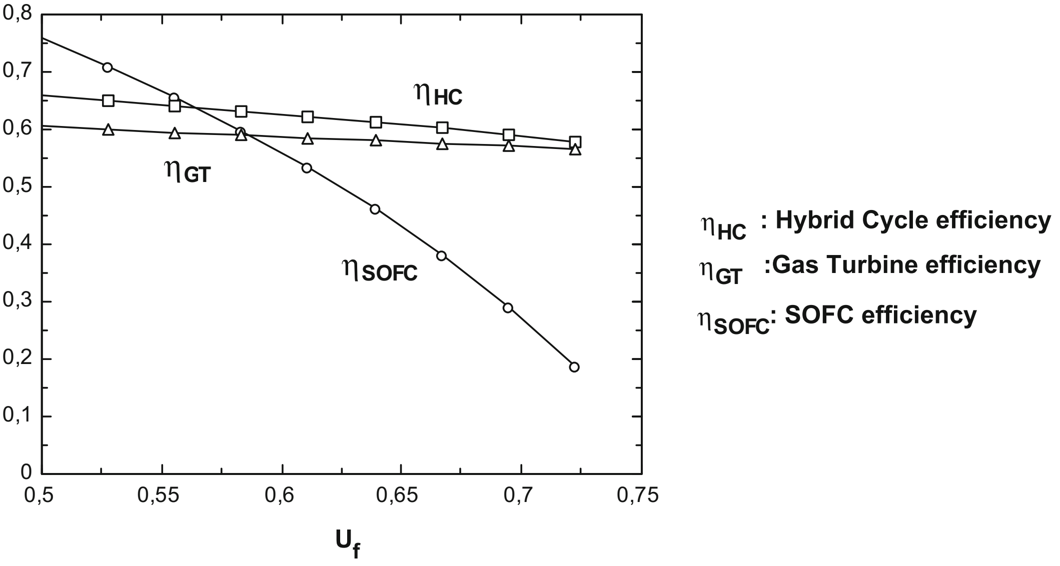

Fig. 6 Effect fuel utilization on system efficiencies

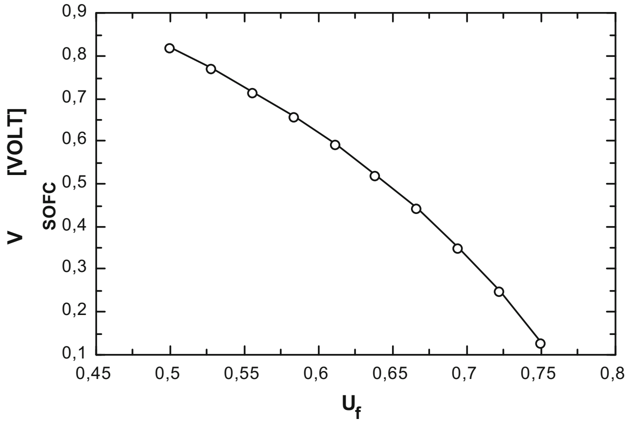

Fig. 7 Effect of fuel utilization factor on SOFC voltage

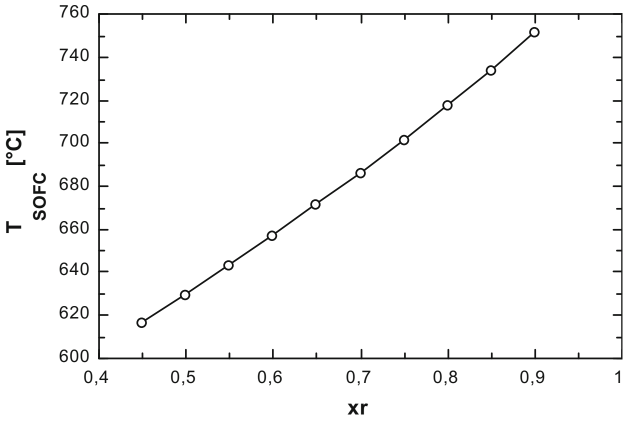

Fig. 8 Effect of pre-reformed fraction on SOFC temperature

the values of the different polarizations. Consequently, the cell voltage increases as shown in Fig. 9.

The variations of the system efficiencies are presented in Fig. 10. For the X_r variation range, the SOFC efficiency increases significantly to reach about 62.5%, while an improvement of about 13% is obtained for the whole system efficiency.

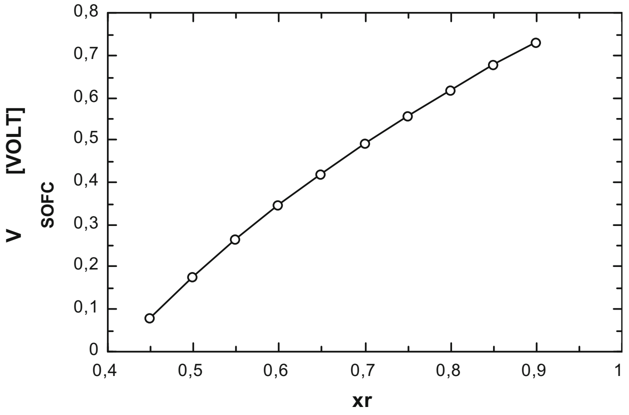

Fig. 9 Effect of pre-reformed fraction on SOFC voltage

5.4 Effect of Air Flow Through the SOFC

Operating at high air flow is essential to avoid the SOFC damage and increase its durability. But, the required air flow depends on the inlet fuel properties. Noting that the SOFC operating with internal reforming requires less air excess than the SOFC supplied with pure hydrogen. In addition, an important air excess may reduce the cell performance because of its temperature drop. On the other hand, the air excess can be beneficial for the cell performance since it increases the Nernst voltage and decreases the activation

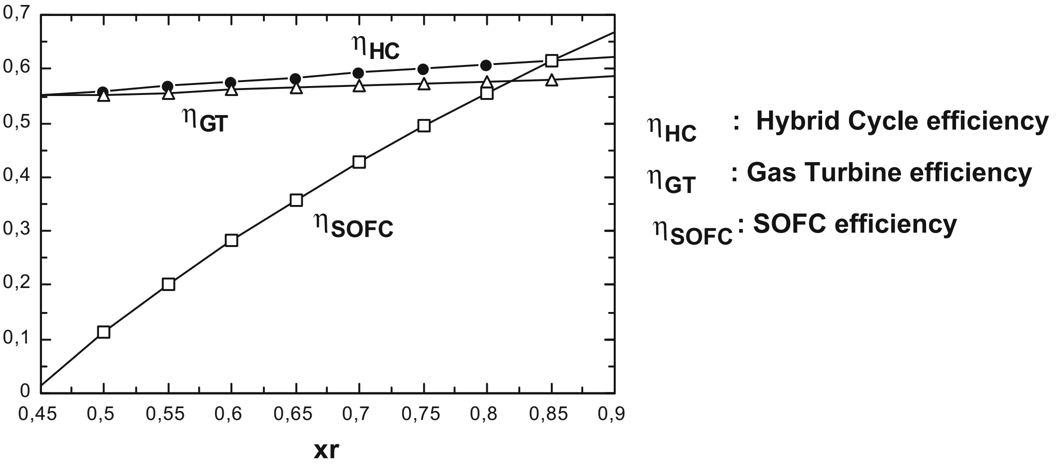

Fig. 10 Effect of pre-reformed fraction on system efficiencies

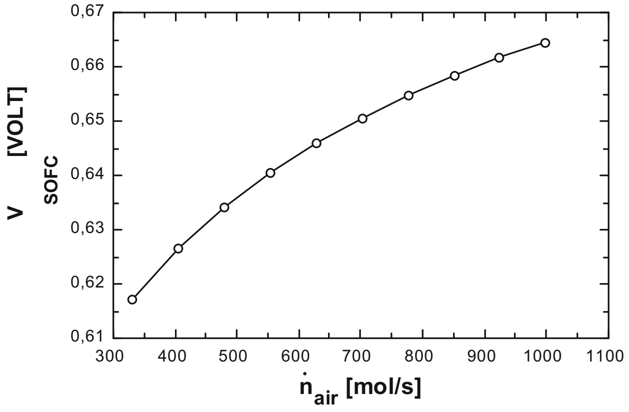

Fig. 11 Effect of air flow on SOFC voltage

and concentration polarizations. Besides, the mass flow rate through the gas turbine will be increased, which improves its performance.

Figure 11 depicts the variation of the cell voltage against the air molar flow rate for pressure ratio, pre-reforming fraction utilization factor of 10, 0.8 and 0.6, respectively. The cell voltage increases of about 8% for a variation range of the air flow from 333 to 1000 mol/s.

The variation of the system performances according to air flow rate is presented in Fig. 12. Despite the increase of the cell voltage presented in Fig. 11, the SOFC efficiency decreases notable with the increase of air flow rate. This is explained by the growing of the SOFC air compressor power consumption. A small improvement is obtained for the gas turbine efficiency. That leads to slight increase in the hybrid cycle efficiency lower than 2%.

6 Conclusions

A performance analysis of a hybrid SOFC–GT power plant was conducted. The natural gas is used as fuel for the SOFC

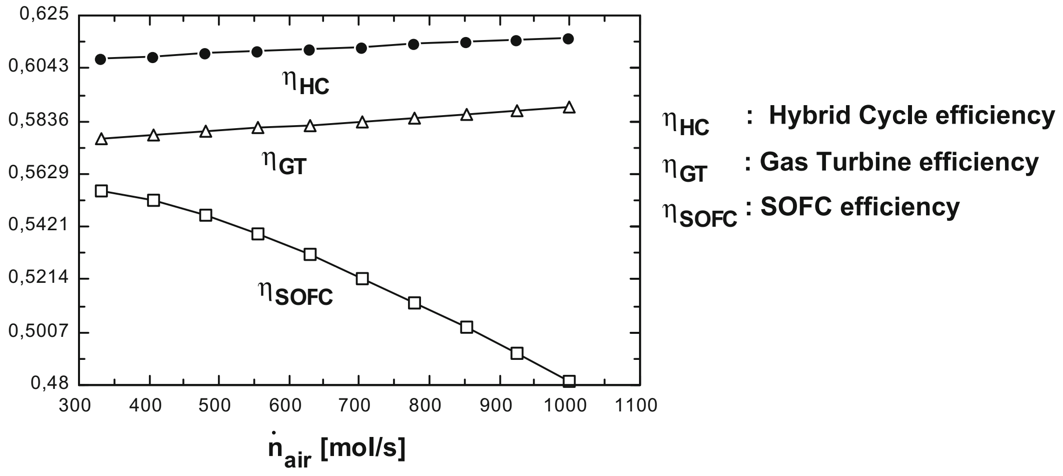

Fig. 12 Effect of air flow through the SOFC on system efficiencies

and the GT cycle. An external pre-reforming system is considered before the SOFC. The CO_2 emissions cannot be neglected due to reforming process. The gas from the SOFC exhaust is used to preheat the GT air compressor outlet. Then, it is injected in the combustion chamber. The gas at the turbine exhaust is used to generate the steam required for the reforming process. The effects of the main operating parameters on the power plant performances are analyzed.

The integration of the SOFC enhances the hybrid cycle efficiency of about 50%. The increase of the ambient temperature reduces the system efficiencies. The utilization factor has a negative effect on the SOFC temperature and voltage which leads to a decrease in the system performances, while the pre-reforming fraction has a positive effect on the indicated parameters.

The SOFC voltage increases with the air molar flow rate. However, required air compressor power becomes important. That reduces significantly the SOFC efficiency. A small improvement of about 2% is obtained for the hybrid cycle efficiency SOFC–GT.

The performance of our cycle may be also enhanced by the integration of CO_2 capturing system and cooling cycle which recovers waste heat from SOFC–GT hybrid system. The optimum system design will be specified using a thermoeconomic analysis. This constitutes the aim of our later paper.

The obtained results may constitute helpful tools to better undertake future investigations on the hybrid power plants.

References

1. Massardo, A.F.; Lubelli, F.: Internal reforming solid oxide fuel cell–gas turbine combined cycles (IRSOFC–GT): part A—cell model and cycle thermodynamic analysis. J. Eng. Gas Turbine Power **122**, 27–35 (2000)
2. Barelli, L.; Bidini, G.; Ottaviano, A.: Part load operation of SOFC/GT hybrid systems: stationary analysis. Int. J. Hydrog. Energy **37**, 16140–16150 (2012)
3. El-Emama, R.S.; Dincera, I.; Naterera, G.F.: Energy and exergy analyses of an integrated SOFC and coal gasification system. Int. J. Hydrog. Energy **37**, 1689–1697 (2012)
4. Horlock, J.H.: Combined power plants: past, present and future. Trans. ASME J. Eng. Gas Turbines Power **117**, 608–616 (1995)
5. Kelhofer, R.: Combined Cycle Gas and Steam Power Plants. Fairmount Press, Inc, Lilburn (1991)
6. Massardo, A.F.; Lubelli, F.: Internal reforming solid oxide fuel cell-gas turbine: part A: cell model and cyclethermodynamic analysis. J. Eng. Gas Turbine Power **122**, 27–35 (2000)
7. Dincer, I.; Rosen, M.; Zamfirescu, C.: Exergetic performance analysis of a gas turbine cycle integrated with a solid oxidefuel cells. J. Energy Resour. Technol. **131**, 1–11 (2009)
8. Saisirirat, P.: The solid oxide fuel cell (SOFC) and gas turbine (GT). Hybrid Syst. Numer. Model Energy Procedia **79**, 845–850 (2015)
9. Yi, Y.; Rao, A.D.; Brouwer, J.; Samuelsen, G.S.: Analysis and optimization of a solid oxide fuel cell and intercooled gas turbine (SOFC–ICGT) hybrid cycle. J. Power Sources **132**, 77–85 (2004)
10. Inui, Y.; Yanagisawa, S.; Ishida, T.: Proposal of high performance SOFC combined power generation system with carbon dioxide recovery. Energy Convers. Manage. **44**(4), 597–609 (2003)
11. Chan, S.H.; Ho, H.K.; Tian, Y.: Modelling of simple hybrid solid oxide fuel cell and gas turbine power plant. J. Power Sources **109**(1), 111–120 (2002)
12. Massardo, A.F.; Lubelli, F.: Internal reforming solid oxide fuel cell-gas turbine combined cycles (IRSOFC-GT): part A-cell model and cycle thermodynamic analysis. J. Eng. Gas Turbine Power **122**, 27–35 (2000)
13. Arsalis, A.: Thermodynamic modeling and parametric study or hybrid SOFC-gas turbine-steam turbine power plants ranging from 1.5 to 10 MWe. J. Power Sources **181**, 313–326 (2008)
14. Ishak, F.; Dincer, I.; Zamfirescu, C.: Energy and exergy analyses of direct ammonia solid oxide fuel cell integrated with gas turbine power cycle. J. Power Sources **212**, 73–85 (2012)
15. Penyarat, C.; Pascal, B.: The hybrid solid oxide fuel cell (SOFC) and gas turbine (GT) systems steady state modeling. Int. J. Hydrog. Energy **37**, 9237–9248 (2012)
16. Zhang, X.; Li, J.; Li, G.; Feng, Z.: Cycle analysis of an integrated solid oxide fuel cell and recuperative gas turbine with an air reheating system. J. Power Sources **164**, 752–760 (2007)
17. Zamfirescu, C.; Dincer, I.: Thermodynamic performance analysis and optimization of a SOFC-H^+ system. Thermochim. Acta **486**, 32–40 (2009)
18. Saebea, D.; Authayanun, S.; Patcharavorachot, Y.; Arpornwichanop, A.: Effect of anode–cathode exhaust gas recirculation on energy recuperation in a solid oxide fuel cell-gas turbine hybrid power system. Energy **94**, 218–232 (2016)
19. Zhang, X.; Li, G.; Li, J.; Feng, Z.: Numerical study on electric characteristics of solid oxide fuel cells. Energy Convers. Manag. **48**, 977–989 (2007)
20. Singhal, S.C.; Kendall, K.: High Temperature Solid Oxide Fuel Cells: Fundamentals Design and Applications. Elsevier, Oxford (2003)
21. Berger, C.: Handbook of Fuel Cell Technology. Prentice-Hall, Englewood Cliffs (1968)
22. Cocco, D.; Tola, V.: Externally reformed solid oxide fuell cell–micro-gas turbine (SOFC–MGT) hybrid systems fueled by methanol and di-methyl-ether (DME). Energy **34**, 2124–2130 (2009)
23. Isfahani, S.N.R.; Sedaghat, A.: A hybrid micro gas turbine and solid state fuel cell power plant with hydrogen production and CO_2 capture. Int. J. Hydrog. Energy **41**, 9490–9494 (2016)
24. Duan, L.; Huang, K.; Zhang, X.; Yang, Y.: Comparison study on different SOFC hybrid systems with zero-CO_2 emission. In: The 25th International Conference on Efficiency, Cost, Optimization and Simulation of Energy Conversion Systems and Processes. ECOS (2012)
25. Chan, S.H.; Ho, H.K.; Tian, Y.: Modelling of simple hybrid solid oxide fuel cell and gas turbine power plant. J. Power Sources **109**, 111–120 (2002)
26. Penoncello, S.G.: Thermal energy systems: design and analysis. International standard book number 576. ISBN 9781482245998